Formation and Dissociation of Rhodamine 800 Dimers in Water: Steady-State and Ultrafast Spectroscopic Study

Kentaro Sekiguchi, Shoichi Yamaguchi, and Tahei Tahara*

Molecular Spectroscopy Laboratory, RIKEN (The Institute of Physical and Chemical Research), 2-1 Hirosawa, Wako, Saitama 351-0198, Japan

Received: September 6, 2005; In Final Form: December 2, 2005

We investigated the fundamental photophysics and photochemistry of a cationic dye rhodamine 800 (R800) in water using steady-state and ultrafast time-resolved spectroscopies. In the ground state, the monomer and dimer coexist in equilibrium, which causes significant concentration dependence of UV−visible (vis) absorption spectra. We determined the equilibrium constant as well as the molar absorption spectra of the monomer and dimer from a global fitting analysis of the UV−vis spectra. The obtained pure dimer spectrum indicates that it is a nonparallel H-dimer. In contrast to the absorption spectra, the steady-state fluorescence spectra do not show any noticeable concentration dependence. The fluorescence lifetime was determined as 0.73 ns regardless of the concentration, and the fluorescence of R800 in water was solely attributed to the monomer. In femtosecond time-resolved absorption measurements, we observed the $S_n \leftarrow S_1$ absorption bands of the monomer and the dimer, as well as the ground-state bleaching signals. It was found that the S_1 dimer dissociates to produce the S_1 monomer (and the S_0 monomer) or relaxes to the S_0 dimer with a time constant of as short as 3.0 ps, which brings about the absence of dimer fluorescence.

Introduction

Dye molecules are widely known as very important materials for science, technology, and industry. From a molecular scientific point of view, fundamental photophysical processes including internal conversion, intersystem crossing, and radiative relaxation can be all observed most typically through the excited-state spectroscopies of dye molecules.[1] From a technological and industrial viewpoint, dye sensitization is extensively exploited in photography, light-energy conversion,[2] photodynamic therapy,[3] and so on. Dyes are also significantly utilized as indicators and laser gain media. All these applications absolutely necessitate the fundamental knowledge of the photophysics and photochemistry of dye molecules that are readily affected by their environments. As regards ionic dyes, for example, association is strongly favored in water.[4−10] The association of dyes brings about considerable changes of the photophysical properties. The excited-state dynamics of associating dyes is sometimes not straightforward because of the presence of multiple transient species. Nevertheless, the recent progress of ultrafast spectroscopies enables us to investigate a variety of complicated photochemical systems.[11−14]

In the present paper, we elucidate the excited-state dynamics of rhodamine 800 (R800) in water using the steady-state UV−visible (vis), picosecond time-resolved fluorescence, and femtosecond time-resolved absorption spectroscopies. R800 is a cationic dye shown in Chart 1. Although not many examples have been reported so far, it can probe hydrogen bonding and solvation dynamics of water.[15] It can even probe chemical reactions in membranes with the advantage of its near-infrared (NIR) absorption.[16] R800 is highly surface active, and fundamental photophysics at water interfaces can also be probed with this molecule. Actually, we studied ultrafast dynamics of this molecule at the air/water interface by femtosecond time-resolved multiplex electronic sum-frequency generation spectroscopy,[17] which will be reported elsewhere.[18]

CHART 1: Molecular Structure of Rhodamine 800

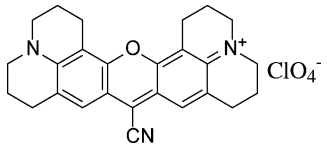

Although the solvation dynamics[15] and the electron-transfer reaction[19] of R800 in solution were already reported, the more fundamental photophysics and photochemistry of R800 have been left open. This paper is constructed as follows: First we unravel the monomer−dimer equilibrium of R800 in the electronic ground (S_0) state using the concentration dependence of the UV−vis spectra. Then we discuss the steady-state fluorescence spectra and fluorescence lifetime and show that the fluorescence is solely attributed to the lowest excited singlet (S_1) state of monomeric R800. Finally, we examine the excited-state dynamics of R800 by femtosecond time-resolved absorption spectroscopy and present a scheme for the relaxation dynamics of the monomer and dimer on the basis of the obtained time-resolved data.

Experimental Section

R800 was purchased from Exciton as LD 800 (perchlorate) and used without further purification. As a spectroscopic sample solution, R800 was dissolved in HPLC-grade distilled water (Wako). Because R800 was sparingly soluble in water, the concentration of the saturated solution was 8.3×10^{-5} mol dm^{-3}. The ground-state UV−vis absorption spectra of R800 in water were measured with a commercial spectrometer (Hitachi, U-3400). Quartz cells of 10 or 100 mm optical path length were used, depending on the sample concentration that ranged from 1.3×10^{-6} to 8.3×10^{-5} mol dm^{-3}.

* Corresponding author. E-mail: tahei@riken.jp.

10.1021/jp055027p CCC: $33.50
Published on Web 02/08/2006

The picosecond time-resolved fluorescence spectroscopy was performed with a femtosecond laser system and a streak camera. The detail of the laser system was described previously.[20] The sample solution in a 1 mm quartz cell was irradiated by a femtosecond pulse at 690 nm. The cell was a 1 mm × 10 mm rectangular parallelepiped. The incident angle between the pump light and the surface normal of the cell was 45°. Fluorescence was collected with a lens that was put in front of the cell (reflection configuration). The light axis of the lens was parallel to the surface normal.

The linear polarization direction of the excitation pulse was vertical. Fluorescence emitted from the sample was collected and focused on the entrance slit of an imaging polychromator (Hamamatsu, C5094). The spectrally dispersed fluorescence was detected by a streak camera (Hamamatsu, C4334) with the time resolution of 25 ps. A polarizer in front of the polychromator was set at the magic angle to acquire fluorescence decay signals free from the rotational relaxation.

The detail of the femtosecond time-resolved pump−probe absorption spectroscopy was described previously.[12] Briefly, the sample solution in the 1 mm cell was photoexcited by a pump pulse at 690 nm, and a continuum probe pulse passing through the irradiated area of the sample was analyzed by a single polychromator (HR-320, Jobin Yvon) equipped with a thermo-electrically cooled CCD (Spec-10:256E, Roper Scientific). A pump-induced change in the probe spectrum was recorded as a function of the time delay between the pump and probe pulses. The cross correlation width of the pump and probe pulses was about 300 fs (fwhm). The pump polarization was set at the magic angle with respect to the probe polarization. Chirp correction was performed by using the optical Kerr effect method to make final results.[21]

All the measurements were performed at room temperature, 299 K.

Results and Discussion

Figure 1 shows the steady-state UV−vis absorption spectra of R800 in aqueous solutions (solid curves). The vertical axis represents absorbance normalized by the molar concentration of R800 and the optical path length. The spectrum for the lowest concentration is shown in Figure 1h. This has two peaks, one at 625 nm and the other at 690 nm. As the concentration increases, the peak height at 625 nm increases and that at 690 nm decreases. This significant spectral change indicates that aggregation takes place effectively at higher concentration. We analyze the observed concentration dependence of the UV−vis spectrum by assuming a monomer−dimer equilibrium, M + M ⇌ D (M and D represent the monomer and dimer of R800, respectively). In this case, each spectrum in Figure 1 is supposed to be reproduced by the linear combination of the molar absorption spectrum of the monomer (ϵ_M) and that of the dimer (ϵ_D) in the following way:

$$A_i = \frac{1}{C_i}([M]_i\epsilon_M + [D]_i\epsilon_D) \tag{1}$$

Here, A_i is the normalized spectrum shown in Figure 1, C_i is the total molar concentration of R800, $[M]_i$ and $[D]_i$ are the molar concentration of the monomer and the dimer, respectively, and the subscript i represents the ith sample. We introduce the equilibrium constant K_{eq} that is defined as $K_{eq} = [D][M]^{-2}$ (the subscript i is omitted because K_{eq} does not depend on (i). On the basis of the relation $C_i = [M]_i + 2[D]_i$ and the definition of

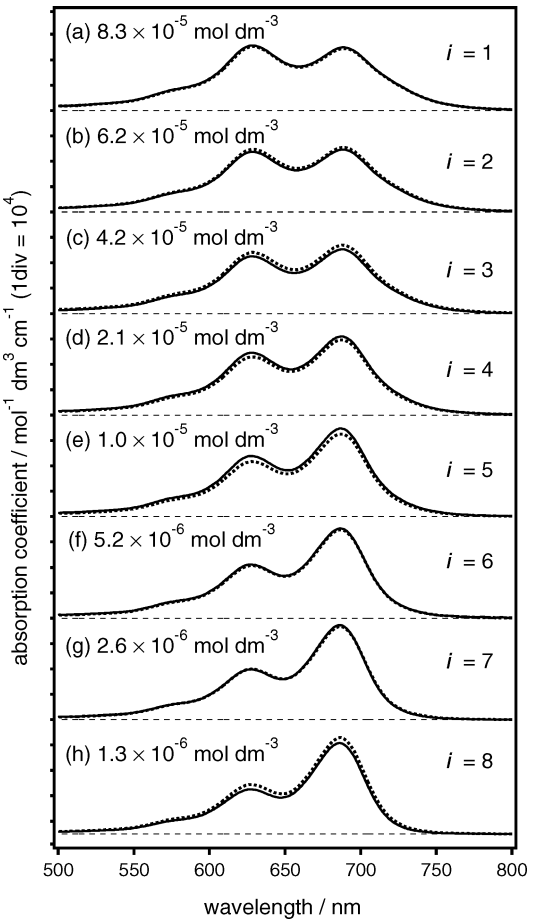

Figure 1. Steady-state UV−vis spectra of R800 in water. The concentrations of solutions (a)−(h) are 8.3×10^{-5}, 6.2×10^{-5}, 4.2×10^{-5}, 2.1×10^{-5}, 1.0×10^{-5}, 5.2×10^{-6}, 2.6×10^{-6} and 1.3×10^{-6} mol dm^{-3}, respectively. The solid curves represent the data, and the dotted curves represent the spectra obtained by the global fitting analysis.

K_{eq}, $[M]_i$ and $[D]_i$ can be written as simple functions of C_i and K_{eq}, as follows:

$$[M]_i = \frac{1}{4K_{eq}}(\sqrt{8C_iK_{eq} + 1} - 1) \tag{2}$$

$$[D]_i = \frac{C_i}{2} - \frac{1}{8K_{eq}}(\sqrt{8C_iK_{eq} + 1} - 1) \tag{3}$$

Although ϵ_M and ϵ_D are unknown, they can be written as the linear combination of two spectra in Figure 1, e.g., A_1 and A_8:

$$\epsilon_M = \alpha_1^M A_1 + \alpha_8^M A_8 \tag{4}$$

$$\epsilon_D = \alpha_1^D A_1 + \alpha_8^D A_8 \tag{5}$$

Treating K_{eq}, α_1^M, α_8^M, α_1^D, and α_8^D as fitting parameters, all the data spectra A_1−A_8 were globally fitted to eq 1 in combination with eqs 2−5. In Figure 1, the fitted curves are shown with dotted curves. All the data are successfully reproduced by the global fitting, which means that the observed concentration dependence of the absorption spectra is fully rationalized by the monomer−dimer equilibrium. The equilibrium constant K_{eq} was obtained as 2.8×10^4 mol^{-1} dm^3. Figure 2 shows the ϵ_M and ϵ_D spectra obtained by the analysis. The area intensity of the dimer ϵ_D spectrum is twice as large as that of ϵ_M, which confirms the reliability of the present analysis. It is seen that

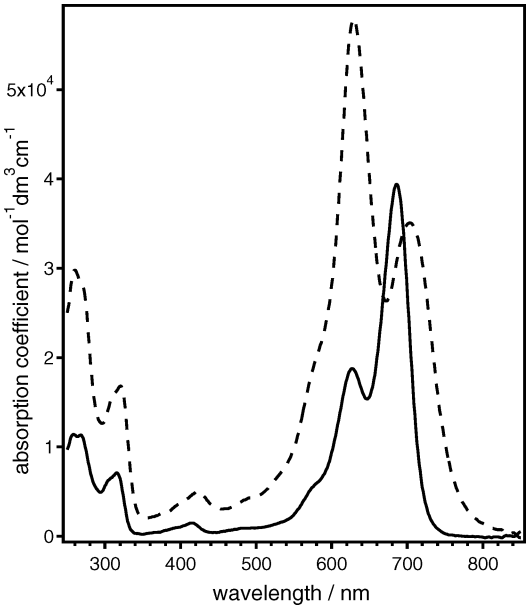

Figure 2. Absorption spectra of the monomer (ϵ_M) and dimer (ϵ_D) of R800 in water. Solid and dashed curves represent the ϵ_M and ϵ_D spectra, respectively.

the strongest absorption band at 686 nm in the monomer ϵ_M spectrum is split into two bands located at 629 and 707 nm in the dimer ϵ_D spectrum. The spectral change upon dimerization can be explained by the exciton coupling theory.[22] Because the stronger peak at 629 nm of ϵ_D is blue-shifted compared with that with the 686 nm band in the ϵ_M spectrum, the dimer can be basically regarded as a so-called H-dimer that is typically found for cationic dyes in water.[23] Because the second transition of the excitation splitting also appears with considerable intensity (i.e., the weaker band around 707 nm), the dimer is considered to be a *nonparallel* H-dimer.

Picosecond time-resolved fluorescence measurements of R800 in the saturated (8.3×10^{-5} mol dm^{-3}) and diluted (6.0×10^{-6} mol dm^{-3}) solutions were carried out using a streak camera. Figure 3a shows the fluorescence spectra integrated in the time range of -0.1 to $+1.3$ ns. In contrast to the significant change in the absorption spectra, the fluorescence spectrum is insensitive to the concentration. Taking account of the concentration dependent self-absorption effect, it can be said that these two spectra are identical.

The fluorescence decay curves integrated in the wavelength range of 750−850 nm are shown in Figure 3b. These two decay curves are well reproduced by a single exponential decay function with a time constant of 0.72 ns for the saturated solution and 0.73 ns for the diluted solution, which means that the two curves are identical within the experimental error. The value 0.73 ns is regarded as the time constant of the fluorescence decay after we round the averaged value 0.725 ns. For the diluted solution, the concentration ratio of the monomer to the dimer ([M]/[D]) is estimated as 7.5, which implies that the fluorescence of the diluted sample is predominantly due to the monomer. For the saturated solution, the [M]/[D] ratio is as small as 1.2, but the spectrum and lifetime of fluorescence are identical with those of the diluted solution. It means that the contribution of the dimer fluorescence is negligible, even in the saturated solution. This is consistent with a general rule that aggregation quenches fluorescence. We will give a reason for the absence of the dimer fluorescence later. Consequently, the time constant of the fluorescence decay, 0.73 ns, is solely ascribed to the lifetime of the S_1 state of the monomer.

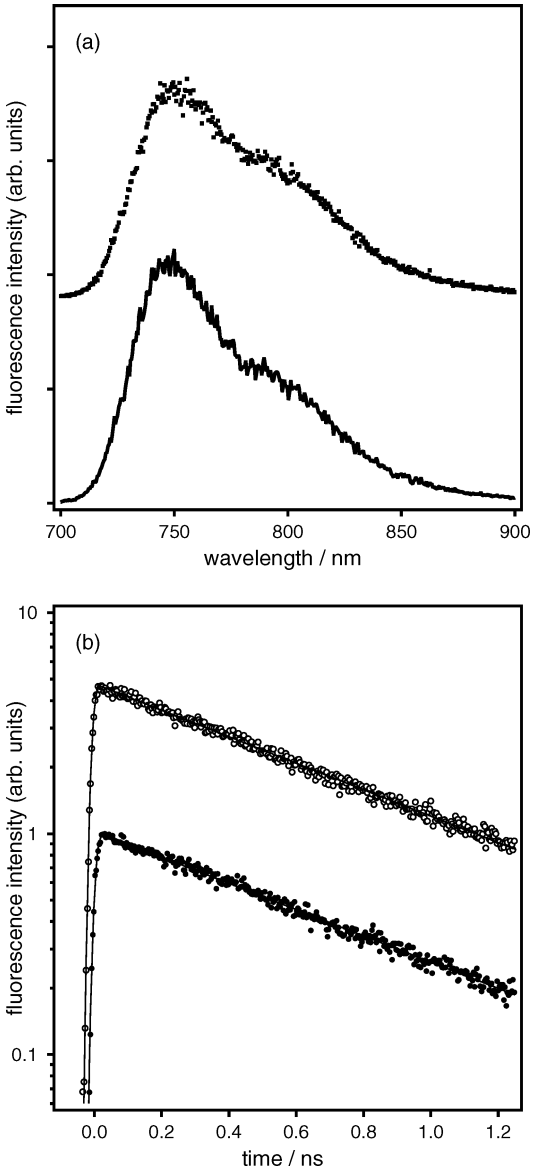

Figure 3. (a) Fluorescence spectra of R800 in water obtained by integrating the time-resolved fluorescence signals from -0.1 to $+1.3$ ns. The dotted and solid lines represent the spectra of the solutions with saturated (8.3×10^{-5} mol dm^{-3}) and diluted (6.0×10^{-6} mol dm^{-3}) concentrations, respectively. The spectral sensitivity calibration of the detector was not performed. The excitation wavelength is 690 nm. (b) Fluorescence decay curves of R800 in water. The open and filled circles stand for the data of the saturated (8.3×10^{-5} mol dm^{-3}) and diluted (6.0×10^{-6} mol dm^{-3}) solutions, respectively. The solid curves represent single-exponential decay functions obtained by the fitting analysis.

Figure 4 shows the femtosecond time-resolved absorption spectra of R800 in water with the saturated concentration. The negative signals around 600−780 nm correspond to the pump-induced decrease of absorbance that is caused by the ground-state bleaching. The band shape of the negative signals changes with the time delay until 10 ps. The negative absorption band after 10 ps is similar to the ϵ_M spectrum (Figure 2) apart from the sign. The positive signals around 500−600 nm are due to the pump-induced increase caused by excited-state absorption. It is seen that the excited-state absorption also changes with delay time until 10 ps. In fact, the peak wavelength of the positive absorption band is about 530 nm until 1 ps, but it is about 590 nm after 10 ps.

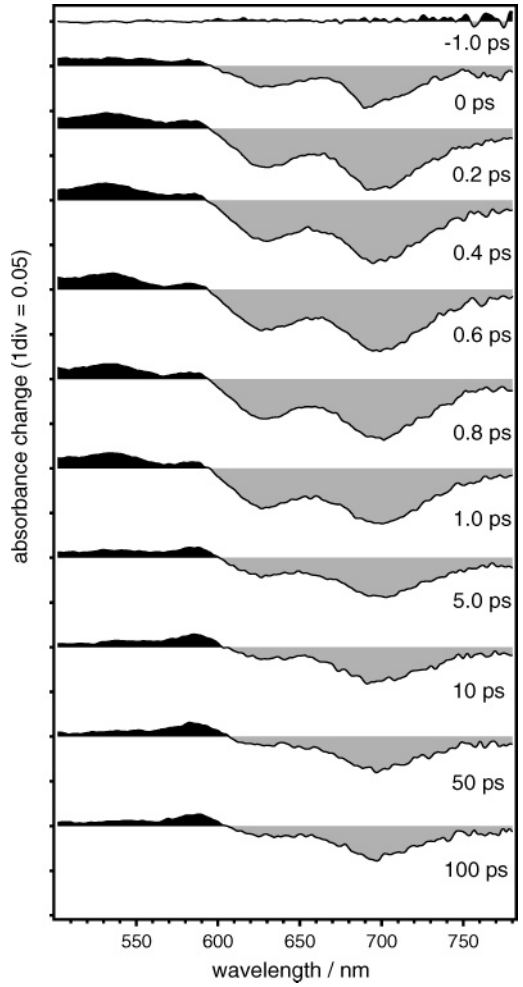

Figure 4. Transient absorption spectra of R800 in water with the saturated concentration (8.3×10^{-5} mol dm^{-3}). The pump wavelength is 690 nm. The time delay between the pump and probe pulses is indicated at the side of each spectrum. The positive and negative signals are represented with the areas painted with black and gray, respectively.

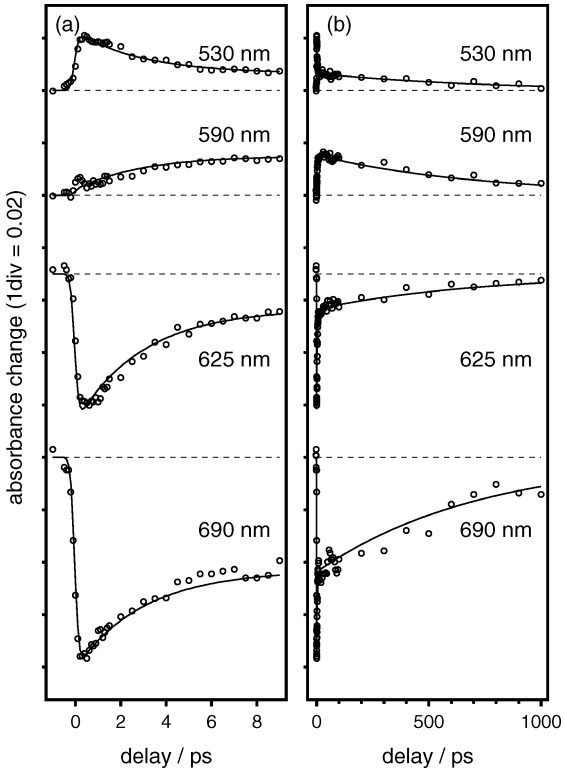

Figure 5. Temporal behavior of the transient absorption signals of R800 in water (8.3×10^{-5} mol dm^{-3}). The data points of the transient spectra shown in Figure 4 were averaged at the center wavelength ±2 nm. The open circles are the data, and the solid lines represent double-exponential decay functions obtained by the fitting analysis. The signals until 9 ps and until 1 ns are shown in (a) and (b), respectively. In the temporal behavior at 590 nm in (a), there is a deviation of the fitting curve from the data around zero time delay. This deviation is due to the inverse Raman scattering signal of water that is not important for the present study.

To quantitatively discuss the excited-state dynamics, we analyzed the time-resolved absorption signals at typical wavelengths shown in Figure 5. In a global fitting analysis using double exponential functions (convoluted with the instrumental response), all the four time-resolved absorption traces were well reproduced. The shorter time constant of the double exponential function was converged at 3.0 ± 0.1 ps, whereas the longer time constant in the range of 0.65−1.0 ns generated successful fits for the slow dynamics. Taking account of the S/N of the signals obtained by the present measurements, we can reasonably identify the longer time constant as the lifetime observed in the picosecond time-resolved fluorescence measurements, which is the S_1 lifetime of the monomer. Therefore, the fitting curves in Figure 5 have been drawn with the longer time constant fixed at 0.73 ns.

The successful global fitting analysis indicates that two distinct dynamics has been observed in the femtosecond time-resolved absorption spectra: the 3 ps and 0.7 ns dynamics. (We use these terms to represent the dynamics that correspond to the lifetimes of 3.0 ps and 0.73 ns, respectively.) The 0.7 ns dynamics is definitely the relaxation dynamics of the monomer in the S_1 state (hereafter abbreviated to S_1(M)). We can recognize relatively large contribution of this 0.7 ns dynamics in the absorption signals at 590 and 690 nm. The positive absorption at 590 nm is straightforwardly assigned to the transient absorption of S_1(M). The negative absorption signal at 690 nm after 10 ps is assignable to the bleaching of the monomer ground state (hereafter abbreviated to S_0(M)). The bleaching signal of S_0(M) decays in accordance with the decay of the transient absorption of S_1(M), which demonstrates that S_1(M) is directly relaxed to S_0(M) with the time constant of 0.73 ns. The 3 ps dynamics, on the other hand, is seen as the rise of the transient absorption of S_1(M) at 590 nm (Figure 5a). This means that (a portion of) the S_1(M) is produced from a transient species that has a lifetime of 3.0 ps. The positive absorption that shows the corresponding 3 ps decay can be found in the signal at 530 nm. Because the monomer and dimer coexist in solution, the photoexcitation generates not only S_1 monomer but also S_1 dimer.[24] Therefore, we attributed the positive absorption at 530 nm to the transient absorption of S_1 dimer (S_1(D)). The 3 ps rise of the S_1(M) signal implies that the relaxation of S_1(D) produces S_1(M). Note that the bleaching signal at 625 nm also shows a substantial decay with the time constant of 3.0 ps. Because the predominant peak of the dimer absorption (ϵ_D) is located around 625 nm (Figure 2), the negative absorption around 625 nm has significant contribution from the bleaching of the S_0 dimer absorption, at least, immediately after photoexcitation. Thus, the 3 ps bleaching recovery at 625 nm is attributed to the recovery of S_0 dimer. Because both the S_0-(D) bleaching recovery at 625 nm and the S_1(M) absorption rise at 590 nm show the 3 ps dynamics, we can conclude that S_1(D) decays with the time constant of 3.0 ps by two relaxation pathways: the dissociation to S_1(M) (plus S_0(M)) and the

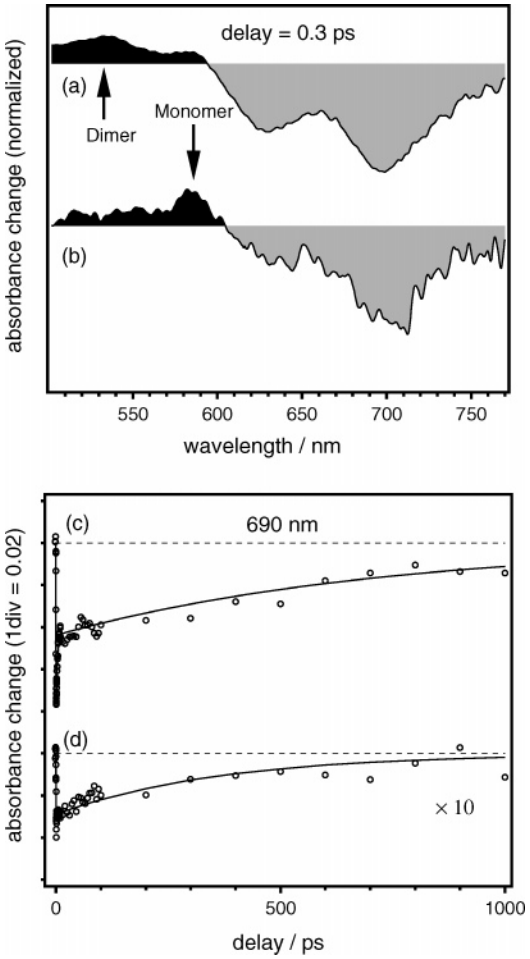

Figure 6. The transient absorption spectra of R800 at 0.3 ps in the (a) saturated (8.3×10^{-5} mol dm^{-3}) and (b) diluted (2.7×10^{-6} mol dm^{-3}) solutions. The pump wavelength is 690 nm. The temporal behaviors of the transient absorption at 690 nm for the saturated and diluted solutions are shown in (c) and (d), respectively. The open circles and solid curve in (c) are the same as those shown in Figure 5b. The data (open circles) in (d) were obtained by averaging the data at 690 nm ± 30 nm. The solid line in (d) represents a single-exponential decay function obtained by the fitting analysis.

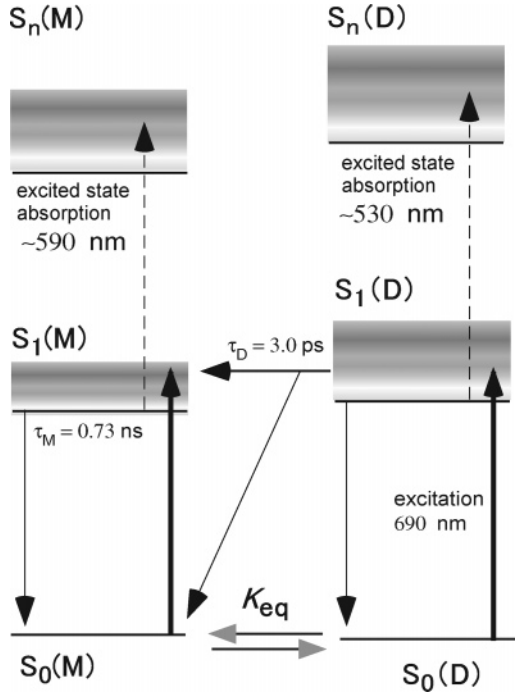

Figure 7. Photophysical and photochemical scheme of R800 in water. The bold arrows represent the excitation process by the pump pulse. The $S_n(M) \leftarrow S_1(M)$ and the $S_n(D) \leftarrow S_1(D)$ absorptions are indicated by dashed arrows. The lifetimes of the $S_1(D)$ and the $S_1(M)$ are 3.0 ps and 0.73 ns, respectively. K_{eq} is the equilibrium constant in the ground state.

relaxation to $S_0(D)$. The absence of the dimer fluorescence is attributed to the very short 3 ps lifetime of $S_1(D)$, which is much shorter than the radiative lifetime of the dimer (0.9 ns, estimated from ϵ_D). Because $S_1(D)$ dissociates into $S_1(M)$, we can conclude that $S_1(M)$ is energetically lower or more stable than $S_1(D)$.

To confirm the assignment of the femtosecond time-resolved absorption, we measured the concentration dependence of the femtosecond time-resolved absorption spectra. Figure 6a and Figure 6b compare the time-resolved spectra at 0.3 ps of the saturated solution (8.3×10^{-5} mol dm^{-3}, [M]/[D] = 1.2) and the diluted solution (2.7×10^{-6} mol dm^{-3}, [M]/[D] = 15). In the time-resolved spectrum of the diluted solution, we cannot clearly see the $S_n \leftarrow S_1$ absorption band of the dimer at 530 nm but undoubtedly discern that of the monomer at 590 nm. In this diluted solution, the concentration ratio of the S_0 dimer is small (~6%), so that $S_1(M)$ is predominantly generated by the direct photoexcitation. On the other hand, the time-resolved spectrum of the saturated solution shows the $S_n \leftarrow S_1$ absorption band of the dimer at 530 nm more distinctly than that of the monomer at 590 nm, because large amount of $S_1(D)$ is generated by photoexcitation. These observations are qualitatively compatible with [M]/[D] of the saturated and diluted solutions, which strongly supports the assignment of the $S_n \leftarrow S_1$ absorption bands of the monomer and dimer. The concentration dependence of the femtosecond time-resolved absorption data is also consistent with the interpretation of the S_0 bleaching dynamics. The bleaching recovery data at 690 nm of the saturated and diluted solutions are shown in Figure 6c,d, respectively. In the data of the diluted solution, the 3 ps dynamics is almost absent, but only the 0.7 ns dynamics is present. This result directly indicates that the 3 ps dynamics is relevant to the dynamics of the dimer whereas the 0.7 ns dynamics is related to the dynamics of the monomer. This directly supports the assignment that the 3 ps dynamics is the relaxation process of $S_1(D)$ and the 0.7 ns dynamics is that of $S_1(M)$.

After $S_1(M)$ generated by the dissociation of $S_1(D)$ decays to $S_0(M)$, the reassociation of $S_0(M)$ must take place in the monomer−dimer equilibration process in the ground state. However, this equilibration process was not identified in the present data. Actually, we did not obtain the time constant of the equilibrium process but only observed the time constants (3.0 ps, 0.73 ns) that were assigned to the lifetimes of $S_1(D)$ and $S_1(M)$. This implies that the equilibration time constant is much shorter than 0.73 ns, which makes it impossible to observe the reassociation of $S_0(M)$ in the equilibration process after the decay of $S_1(M)$. Because dye molecules in water cannot diffuse more than 1 nm within 1 ns (the diffusion coefficient is on the order of 10^2 μm^2 s^{-1}), this reassociation process must be geminate.

Liu et al. investigated the excited-state dynamics of rhodamine 700 (R700) monomer in organic solvents by the fluorescence depletion technique.[25] They found 333 fs and 1.84 ps decay components that were assigned to the intramolecular vibrational energy redistribution and the vibrational cooling, respectively. We can think that R800 may also show temporal absorption changes that reflect these vibrational relaxation processes, because the molecular structure of R700 is similar to that of R800. However, the transient absorption spectra of R800 did

not show any band broadening or peak shift that could be caused by substantial vibrational excess energy. Actually, the transient absorption data were perfectly explained by assuming the two time constants, i.e., the lifetimes of the monomer and dimer in the S_1 state. Therefore, we conclude that the vibrational relaxation processes do not significantly influence the transient signals of R800 in water that was observed in the present femtosecond time-resolved absorption and picosecond time-resolved fluorescence measurements.

In summary, Figure 7 sketches the scheme of the photophysics and photochemistry of R800 in water. The monomer and the dimer are equilibrated with the equilibrium constant K_{eq} ($=2.8 \times 10^4$ mol^{-1} dm^3) in the ground state. In the case of the saturated solution (8.3×10^{-5} mol dm^{-3}), the ratio between the monomer and dimer is estimated as [M]/[D] $= 1.2$. With the photoexcitation at 690 nm, both the monomer and dimer are photoexcited, and S_1(M) and S_1(D) are generated. The lifetime of S_1(D) is as short as 3.0 ps, and S_1(D) is dissociated to S_1(M) and S_0(M), or relaxed to the dimer ground state. After the decay of S_1(D), only the S_1(M) remains and it decays to the S_0 state with the lifetime of 0.73 ns, either radiatively or nonradiatively. Because of the very short lifetime of the S_1(D), its fluorescence can be observed only immediately after photoexcitaion. Therefore, the fluorescence observed is practically assignable to S_1(M). The present scheme provides fundamental knowledge to understand more complicated photochemical dynamics of R800 in different circumstances and to find out potential applications as an environment-sensitive NIR fluorescent dye.

References and Notes

(1) Glasbeek, M.; Zhang, H. *Chem. Rev.* **2004**, *104*, 1929.
(2) Schnadt, J.; Brühwiler, P. A.; Patthey, L.; O'Shea, J. N.; Södergren, S.; Odelius, M.; Ahuja, R.; Karis, O.; Bässler, M.; Persson, P.; Siegbahn, H.; Lunell, S.; Mårtensson, N. *Nature* **2002**, *418*, 620.
(3) Ramaiah, D.; Eckert, I.; Arun, K. T.; Weidenfeller, L.; Epe, B. *Photochem. Photobiol.* **2002**, *76*, 672.
(4) Slavnova, T. D.; Chibisov, A. K.; Görner, H. *J. Phys. Chem. A* **2002**, *106*, 10985.
(5) Abbott, L. C.; Batchelor, S. N.; Oakes, J.; Smith, J. R. L.; Moore, J. N. *J. Phys. Chem. B* **2004**, *108*, 13726.
(6) Neumann, B. *Langmuir* **2001**, *17*, 2675.
(7) Baraldi, I.; Caselli, M.; Momicchioli, F.; Ponterini, G.; Vanossi, D. *Chem. Phys.* **2002**, *275*, 149.
(8) Martínez, V. M.; Arbeloa, F. L.; Prieto, J. B.; López, T. A.; Arbeloa, I. L. *J. Phys. Chem. B* **2004**, *108*, 20030.
(9) Caselli, M.; Latterini, L.; Ponterini, G. *Phys. Chem. Chem. Phys.* **2004**, *6*, 3857.
(10) Das, S.; Thanulingam, T. L.; Thomas, K. G.; Kamat, P. V.; George, M. V. *J. Phys. Chem.* **1993**, *97*, 13620.
(11) Fujino, T.; Arzhantsev, S. Y.; Tahara, T. *Bull. Chem. Soc. Jpn.* **2002**, *75*, 1031.
(12) Takeuchi, S.; Tahara, T. *J. Chem. Phys.* **2004**, *120*, 4768.
(13) Mizuno, M.; Yamaguchi, S.; Tahara, T. *J. Phys. Chem. A* **2005**, *109*, 5257.
(14) Pal, S. K.; Peon, J.; Bagchi, B.; Zewail, A. H. *J. Phys. Chem. B* **2002**, *106*, 12376.
(15) Zolotov, B.; Gan, A.; Fainberg, B. D.; Huppert, D. *Chem. Phys. Lett.* **1997**, *265*, 418.
(16) Sakanoue, J.; Ichikawa, K.; Nomura, Y.; Tamura, M. *J. Biochem.* **1997**, *121*, 29.
(17) Yamaguchi, S.; Tahara, T. *J. Phys. Chem. B* **2004**, *108*, 19079.
(18) Sekiguchi, K.; Yamaguchi, S.; Tahara, T. Manuscript in preparation.
(19) Pugžlys, A.; den Hartog, H. P.; Baltuška, A.; Pshenichnikov, M. S.; Umapathy, S.; Wiersma, D. A. *J. Phys. Chem. A* **2001**, *105*, 11407.
(20) Yamaguchi, S.; Tahara, T. *Chem. Phys. Lett.* **2003**, *376*, 237.
(21) Yamaguchi, S.; Hamaguchi, H. *Appl. Spectrosc.* **1995**, *49*, 1513.
(22) Kasha, M.; Rawls, H. R.; El-Bayoumi, M. A. *Pure Appl. Chem.* **1965**, *11*, 371.
(23) Steinhurst, D. A.; Owrutsky, J. C. *J. Phys. Chem. B* **2001**, *105*, 3062.
(24) The instantaneous rise of the S_1(M) absorption corresponding to the direct photoexcitation is not clearly seen in the transient signals at 590 nm. It is because the negative bleaching signal cancels out the positive signal contribution at the wavelength region.
(25) Liu, J. Y.; Fan, W. H.; Han, K. L.; Deng, W. Q.; Xu, D. L.; Lou, N. Q. *J. Phys. Chem. A* **2003**, *107*, 10857.